Zeitschrift für Geophysik, 1972, Band 38, Seite 701-717. Physica-Verlag, Würzburg

Energetic Protons at Low Equatorial Altitudes

J. MORITZ, Kiel[1])

Eingegangen am 11, April 1972

Summary: Protons in the energy range 0.25 to 1.65 MeV have been measured with a solid state detector telescope onboard the German Research Satellite Azur at equatorial latitudes below the radiation belt. The protons with intensities up to 200 p/cm^2 sec ster exhibit a soft spectrum. Their existence is explained by charge exchange processes in the exosphere and upper atmosphere by which protons that are lost from the outer radiation belt are regenerated at low altitudes. The coupling of the low altitude population to the outer radiation belt population is clearly shown in the flux enhancements that both populations suffer from a magnetic storm event.

Zusammenfassung: Mit dem Experiment EI-92 des Forschungssatelliten Azur wurden bei äquatorialen Perigäumspassagen niederenergetische Protonen im Energiebereich 0,25-1,65 MeV gemessen. Die Protonen wurden in Höhen gemessen, die niedriger sind als die untere Grenze des gut bekannten Van Allen Strahlungsgürtels; dies bedeutet, daß für ihre zeitliche Existenz die Möglichkeit, eine voile Driftbahn um die Erde zu verfolgen, nicht gegeben ist und offensichtlich auch nicht notwendig ist. Die niederenergetischen Protonen werden lediglicit in eager Nachbarschaft zum geomagnetischen *B* = *B*min - Äquator gefunden; dort zeigt ihre Intensität keine nennenswerte Höhen-, Längen- oder L-Abhängigkeit. Erklärt wird diese Protonenpopulation in geringen Höhen als eine Folge der Verluste der Protonen-population des äußeren Strahlungsgürtels durch Ladungsaustauschprozesse, die einen Fluß energetischer Wasserstoff-Atome hervorrufen. In der äußeren Atmosphäre wird dieser Wasserstoff-Fluß wiedenim durch Ladungsaustauschprozesse in Protonen zurückgewandelt. Eine grobe quantitative Abschätzung zeigt, daß das Protonenreservoir des äußeren Strah-lungsgürtels ausreicht, die beobachteten Protonenintensitäten in geringen Höhen aufrecht-zuerhalten. Das steile Energiespektrum und eine Intensitatsänderung in dieser Population von 45 auf 200 Protonen/cm^2 sec ster. infolge des magnetischen Sturmereignisses vom 8. März 1970 verdeutlicht die enge Kopptung mit dem äußeren Strahlungsgürtel, dessen Intensität im Verlaufe dieses Ereignisses ebenfalls erhöht wurde.

Introduction

The well known Van Allen Belt consists of charged particles stably trapped in the earth's magnetic field. Stable trapping occurs as long as the particles in question can complete at least one full drift path around the earth. At low altitudes the Van

[1]) Dr. J. MORITZ, Institut fur Reine und Angewandte Kernphysik der Christian-Albrechts-Universität, 23 Kiel, Olshausenstr. 40-60.

Allen Belt terminates at the innermost *L*-shell that allows the particles (depending on particle energy and species) to complete a drift without being lost from the radiation belt through interactions with the earth's atmosphere. Stated differently, as soon as there are no sources to balance the losses the radiation belt ceases to exist. For protons of the Van Allen Belt this occurs at about $L = 1.15$ for the highest energies through the strong loss processes that the protons encounter in the denser atmosphere of the South Atlantic Anomaly on their drift path around the earth. Here the drift shell $L = 1.15$ comes down to 400 km height. As the atmospheric loss processes (ionization and charge exchange) are of different relative importance depending on the proton energy and the composition of the atmosphere, there is no clearly defined lower boundary for radiation belt protons that is the same for all energies. Lower energy protons are lost at greater heights. The boundary at $L = 1.15$ is valid for the highest trapped proton energies. Below this *L*-value no energetic trapped protons are expected, but only very high energy protons from the cosmic ray background.

Contrary to this expectation, energetic protons have been detected with a solid state detector telescope onboard the satellite GRS-A/Azur well below $L = 1.15$. Within the energy range 0.25— 1.65 MeV the measured intensities are from 70 to 200 p/cm^2 sec ster. The observed protons are narrowly confined to the $B = B_0$ equatorial regions. They most probably constitute a radiation belt around the earth with features that are quite different from those of the Van Allen Belt, although the two are closely related — this will be proposed and elaborated later — since the Van Allen Belt of stable trapped protons acts as a source for this low altitude proton population and in a way this low altitude belt is a copy of the outer Van Allen Belt. Prominent differences are to be seen in a completely different spatial distribution, in the relative independence of the earth's atmosphere, and in the failure of the third adiabatic invariant due to the short lifetimes of the protons (and from this the high importance of the source distribution for the proton distribution). In addition this low altitude population has a differential energy spectrum different from what is known as yet of the adjoining inner Van Allen Belt.

The Experiment

Satellite and orbit

The German Research Satellite Azur was launched Nov. 8, 1969 into a nearly polar orbit of 103° inclination with initial apogee altitude of 3145 km, perigee altitude of 384 km, and orbital period of 122 min. The orbital plane is nearly sun-synchronous and lies in the dawn-dusk plane of the earth. The satellite is magnetically aligned to the earth magnetic field lines. The active lifetime of Azur lasted from Nov. 8, 1969 until June 29, 1970. An onboard tape-recorder capable of storage of two orbits' data failed to operate Dec. 9, 1969. From this date on real-time data only have been received.

Solid state detector telescope EI-92

The proton telescope EI-92 onboard the satellite Azur consists of two totally depleted silicon solid state detectors of equal size, 34 microns thick and 7 mm in diameter. 4 energy threshold discriminators for detector 1, and 1 energy threshold for detector 2, set to the same level as the lowest threshold of detector 1, define in combination with anticoincidence conditions 6 experimental channels whose characteristics are given in Table I.

An acceptance cone for the incoming particles is defined by a mechanical collimator with 20.4° full opening angle. This collimator contains a permanent magnet keeping electrons with energies up to 500 keV from hitting the detectors. The geometric factor of the telescope is 0.0137 cm^2 ster. The axis of the collimator points perpendicular (±5°) to the local magnetic field vector so that the telescope is receiving particles whose pitch angles are 90° ±15°.

Table I

Channel 1:	protons in the energy range 1.65 —13.5 MeV
Channel 2:	protons in the energy range 0.25— 12.5 MeV
Channel 3:	protons in the energy range 0.25 — 1.65 MeV
Channel 4:	protons in the energy range 0.5 — 1.65 MeV
Channel 5:	protons in the energy range 1.0 — 1.65 MeV
Channel 6:	alphas in the energy range 2.0 - 6.4 MeV

The counts in the individual channels are accumulated for a period of 9.875 sec onboard the satellite and transmitted to ground in real-time in 10 sec intervals.

Observations

During the first weeks of operation the perigee of the satellite was in a position such that most evening passes of the satellite lay beneath the Van Allen Belt. As the onboard tape-recorder was still in operation there was good data coverage of these low altitude low latitude passages. All of these passes show a count rate increase in the channels that respond to 0.25—1.65 MeV protons narrowly confined to the region of the $B = B_0$- equator. The absolute count rate of 10 counts/10 sec at the maximum of these intensity increases shows within the limits of statistics no dependence on longitude, altitude (range 400 to 1000 km), nor *L*-value (range 0.99 to 1.14), Fig. 1 shows several equatorial passes at different positions in space that illustrate this independency.

HOVESTADT [1971] was able to confirm the existence of an enhanced count rate at low *L*-values at the equator from the data of the proton telescope EI-88 onboard the same satellite for passes when this telescope which normally covered the energy range 1.5 to 104 MeV was, due to an internal logic, sensitive to protons down to 0.75 MeV. As the solid state detectors of the telescope EI-88 are shielded by a $8.9 \cdot 10^{-4}$ g/cm^2 nickel foil whereas the shielding of the first EI-92 detector consists

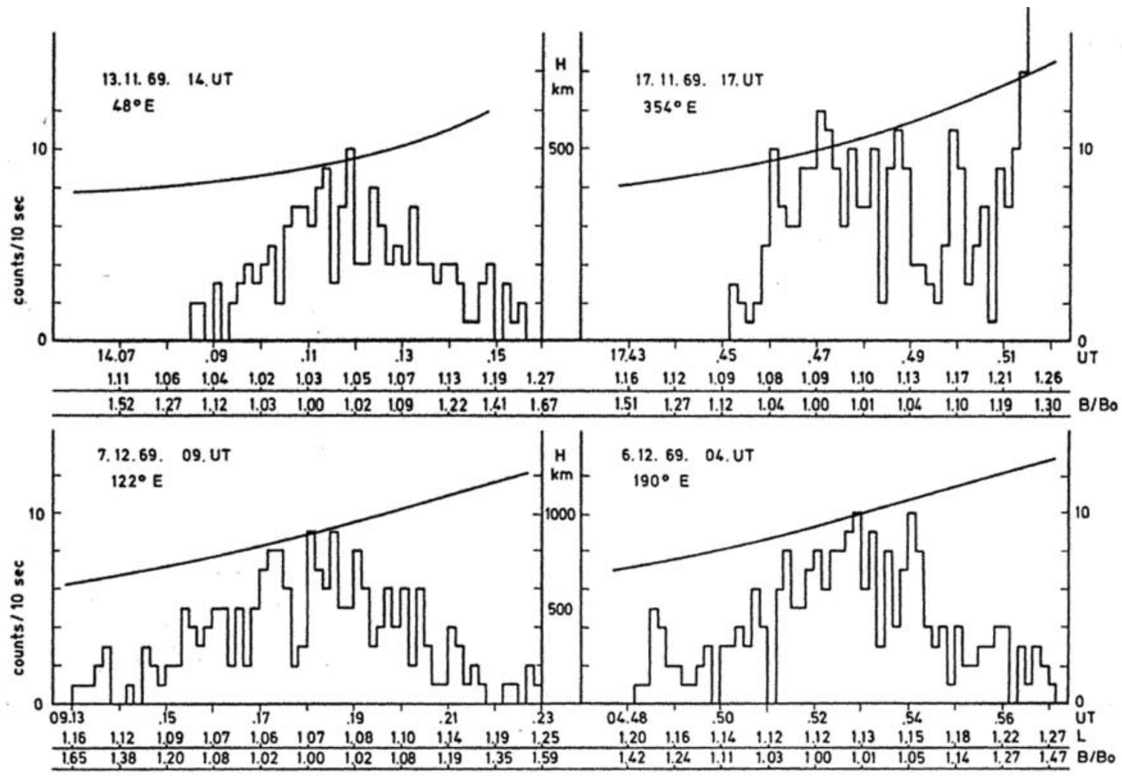

Fig. 1: Count rate profiles (channel 3: E_p: 0.25 — 1.65 MeV) of four equatorial passages of the satellite with *L*-values below 1.15. The passages are from different geographical longitudes, different *L*-values at the equator (given below each plot) and altitudes (given by the curved line in the graphs with scale in-between each two passages). In the passage of 17.11.1969 17. UT the satellite's encounter with the inner radiation belt shortly after the equator passage at 17.51 h causes the steep rise in count rate.

only of the 1.3•10^{-4} g/cm^2 aluminum evaporation onto the solid state detector the consistancy of the intensities between the two telescopes clearly indicates that the observed count rates are due to protons. Havier ions should deposit considerably more energy within the EI-92 detector system than is registered as soon as they become detectable with the EI-88 telescope.

During the first period of the satellite's operation these protons could be seen at local evening only due to the satellite's orbital characteristics. By January 1970 the perigee had moved to local morning and the same effect could be seen on the morning side also. Due to the failure of the tape-recorder only very few low altitude low latitude passes have been obtained but again all of these passes show the existence of the proton population at the $B = B_0$ equator. As the population is closely concentrated around the equator the equatorial intensities plotted against L give a good insight to the peculiar distribution. This is given in fig. 2 showing the constant count rate over the total L-range from 0.99 to 1.14 at which point she count rate starts to rise steeply due to the lower edge of the high energy proton radiation belt. The high energy protons cause a background count rate in all channels of the experiment as they are able to penetrate the detector shielding.

Due to the sun-synchronization of the orbital plane there are no data other than from local morning and evening hours. So no exact statement can be made from the data on whether the proton population realy exists all around the earth.

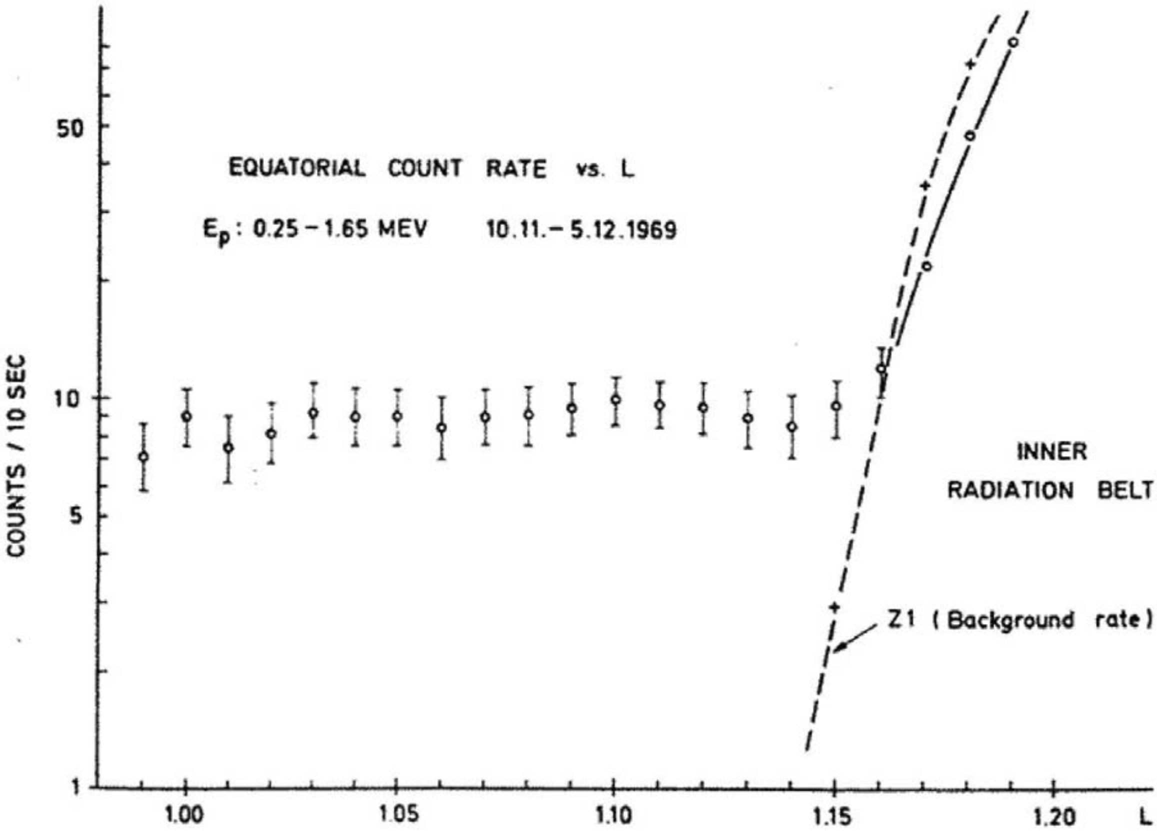

Fig. 2: Maximum equatorial count rates of channel 3 (E_p: 0.25-1.65 MeV) for the time period 10. 11.-5. 12. 1969 for different L-values.

From the channels 3—5 of the experiment a proton differential energy spectrum can be constructed which is shown in fig. 3. There are only small variations to this steep energy spectrum within the first month of operation of which the given spectrum is a mean value. The striking feature of the spectrum is the dominance of low energy protons in contradiction to all that is known about the proton spectra of the adjoining inner radiation belt [MORJTZ 1971].

Discussion of the observations

The observed protons cannot be in the state of stable trapping in the sense of radiation belt protons as they are not able to complete a full drift path around the earth. Taking 350 keV as a representative energy for the observed protons, their lifetimes at least up to a height of 1000 km are considerably shorter than their drift period which is in the order of 7000 sec. Nevertheless they are trapped in respect to their bounce motion behaving like ordinary radiation belt particles.

The important features of the observed proton distribution are its independence of the height of observation and the strong concentration at the $B = B_0$ equator which implies a pitch angle distribution that is sharply peaked at 90 degrees local pitch angle.

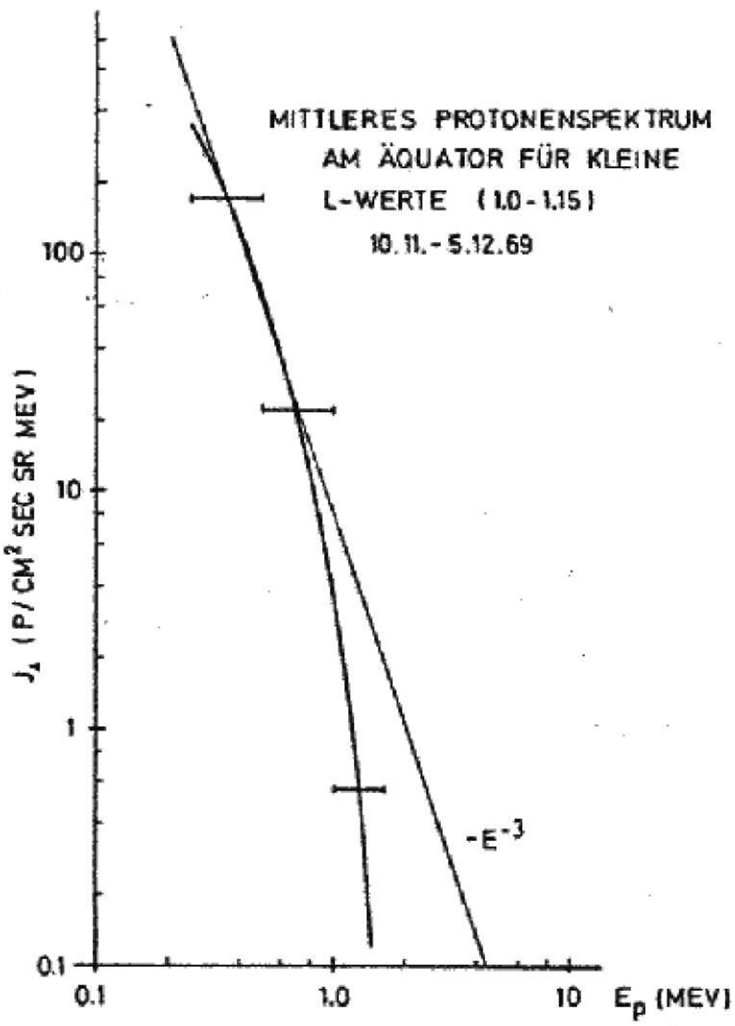

Fig. 3: Average differential proton spectrum seen in the low altitude belt for the time period 10. 115. 12. 1969.

Because the observed proton intensities are independent of the atmospheric density — which should be the controlling factor of their lifetime — it is implied that the source for the protons that counterbalances the atmospheric density determined losses must also be atmospheric density dependent. Furthermore the source geometry must be such that it explains the presence of protons at 400 km height at the equator and yet their absence at 1000 km height for off-equator points where the atmosphere determined lifetime is 10000 times the lifetime at 400 km. This must be an effect of the spatial source function. It is proposed that the necessary source is given by the charge exchange process H* + O => p* +O^- (the star indicating the energetic particle) with the energetic H^-neutrals originating in the outer radiation belt through the charge exchange process p* + H => H* + p.

The first assumption leads to the height independent intensity as long as the H* flux suffers no appreciable attenuation, as then sources and losses are both proportional to the atmospheric density. The second assumption leads to a special source geometry which is given by the proton distribution in the outer radiation belt. This generates a source strongly anisotropic in pitch angle peaked at 90 degrees at the equator.

The basic idea then for the explanation of the observed protons is that in spite of their short lifetimes there is a source of sufficient strength to sustain a temporary stable population. Protons that are lost from the outer radiation belt through charge exchange form an energetic Hydrogen flux that spreads freely in space as the motion of the neutral Hydrogen is uneffected by the magnetic field. As the charge exchange process does not alter any other particle characteristics but the state of charge the source distribution for the H-neutrals at the point of generation can be considered as equal to the observed proton distribution with the absolute magnitude given by the appropriate charge exchange cross section. As soon as the inverse charge exchange process occurs the fast particle (once again a proton) will become trapped again in the earth's magnetic field and is detectable as a trapped proton population.

In order to estimate the effectiveness of a first simple model of this process, it is assumed that the protons in the outer radiation belt are lost through charge exchange with the thermal hydrogen exosphere and that they are regenerated at the low altitude locations through charge exchange with oxygen taken to be the main constituent of the high atmosphere. They are eventually lost again through charge exchange with oxygen also.

Ionization losses will be neglected in this first approximation as the lifetime against such losses at the points of measurement is generally longer than the lifetime determined by the charge exchange process.

A rough estimate is the following. An equatorial ring of certain L-value in the outer belt will roughly contribute to the H* flux at a point at low altitude at the equator in proportion to the part of this ring that can be seen by the low altitude point. If this is taken to be about 30% and if an average flux of equatorial mirroring protons with 250 keV of 10^7 p/cm^2 sec ster is taken for an *L*-range of 2.5 to 3.5, then each *L*-ring of 1 cm^2 cross section will contribute a H* flux of $0.3 \cdot 10^7 \cdot 10^{-18} \cdot 500$ H*/cm^2 sec ster, where 10^{-18} cm^2 is the charge exchange cross section for loss of protons from the outer belt and 500 H/cm^3 is the average density of exospheric hydrogen. As there are $6.37 \cdot 10^8$ such rings between 2.5 and 3.5 *L* the estimate of the H* flux at a low altitude point leads to

$$6.37 \cdot 10^8 \cdot 0.3 \cdot 10^7 \cdot 10^{-18} \cdot 500 \approx 1 \text{ H*/cm}^2 \text{ sec ster at 250 keV.}$$

This H* flux is converted to a proton flux in proportion to the ratio of the cross sections for the generation and loss of protons through charge exchange with oxygen; this ratio is about 40 at 250 keV. Thus this estimate leads to a trapped proton flux mirroring at the equator at low altitudes of 40 p/cm^2 sec ster, which is a reasonable number compared to the measurements encouraging a more quantitative calculation.

Quantitative Calculations

1. If there is a H* flux this will be attenuated by charge exchange with the constituents of the atmosphere. The maximum cross section for any atmospheric constituent and a 350 keV hydrogen atom is in the order of 10^{-17} cm^2 per atmospheric atom or molecule. So the H* flux is certainly not attenuated down to an atmospheric depth of 10^{15} n/cm^2, which is about the depth at 400 km height. This is a crude estimate but it is on the pessimistic side and shows that the primary source quantity, i.e. the fast Hydrogen flux, is independent of height within the range covered by the measurements.

2. In order to test the validity of the proposed source numerically the H* flux and flux distribution resulting from the charge exchange losses of protons from the outer radiation belt have been calculated using a simple model of the proton intensity distribution in the outer belt. The equatorial distribution of the perpendicular proton flux that was used in these calculations is shown in fig. 4 together with the distribution of the radiation belt population model AP-5 of KING [1967]. For off-equatorial points a B/B_0 dependency was introduced in the form

$$j_\perp(L, B/B_0) = j_\perp(L, 1)/(B/B_0)^{(5.5-L)},$$

which is in agreement with data of this experiment at off-equator locations in the outer belt and approximating the AP-5 model.

Taking this model of the proton population, considering the radiation belt's geometry to be symmetric about the earth's dipole axis, and using an exospheric thermal neutral hydrogen density in the form

$$n^H = 10^5 \cdot R_E^{-4.25},$$

which is an approximation to the KN-M model given by MEIER [1970], the fast Hydrogen flux at low L points in the equatorial plane resulting from the outer belt protons mirroring at the equator was calculated by numerical integration over the outer belt within the limits $1.5 \leq L \leq 4.5$. The result obtained is that a unit proton flux per cm^2•sec•ster•MeV of equatorial mirroring protons at the maximum of the assumed distribution at $L = 3$ leads to a Hydrogen flux at $L = 1.1$ at the equator of

$$N_H(E) = 0.5 \cdot 10^{12} \cdot \sigma_{10}^{H}(E) \quad H^*/cm^2 \text{ sec ster MeV}.$$

$\sigma^{H}_{10}(E)$ is the cross section for the charge exchange process p* + H => H* + p. Within the energy range 0.25—1.65 MeV this cross section can be approximated by

$$\sigma_{10}^{H}(E) = 1.7 \cdot 10^{-22} \cdot E^{-5.7} \quad cm^2.$$

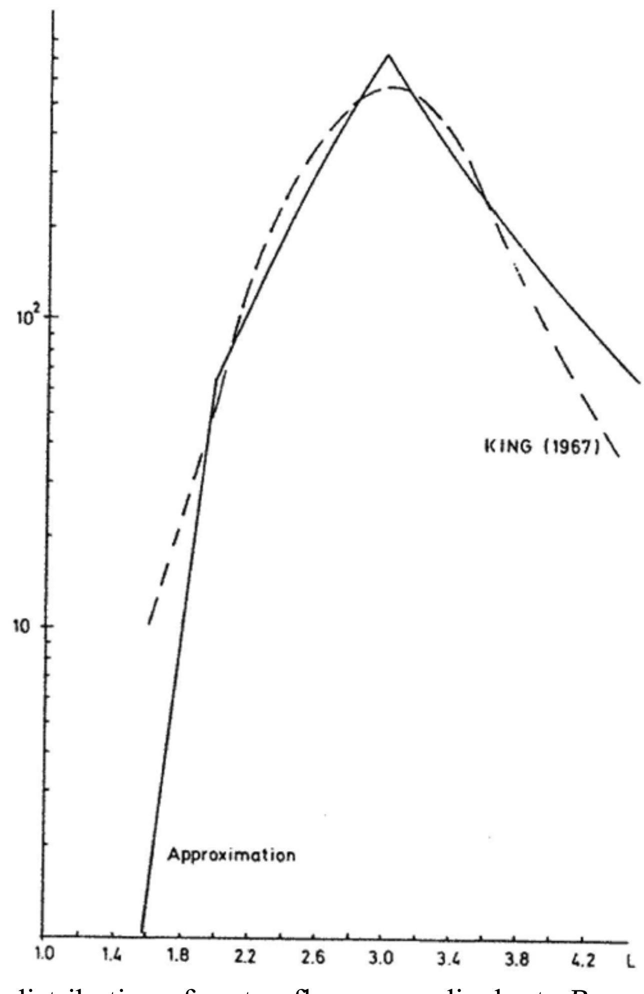

Fig. 4: The equatorial distribution of proton flux perpendicular to B used in the calculations in comparison with the distribution of the model AP-5 given by KING [1967] (dashed line) in relative units.

The values for the cross sections that are used are taken from a compilation of charge exchange cross sections given by TOBUREN et al. [1968].

At the low altitude point the charge exchange processes H* + O => p*+O^- or p* + O + e with cross section σ^O_{01} for the generation of protons, and p* + O => H* + O^+ with cross section σ^O_{10} for the loss of protons are considered. The equation describing the process at the low altitude point is:

$$\frac{dN_p(E)}{dt} = v \cdot n^0 \cdot \sigma^0_{01}(E) \cdot N_H(E) - v \cdot n^0 \cdot \sigma^0_{10}(E) \cdot N_p(E),$$

where n^0 is the number of atmospheric oxygen atoms per cm^3, $N_p(E)$ the differential proton flux, $N_H(E)$ the differential hydrogen flux and v the proton or hydrogen velocity. Considering $N_H(E)$ as temporarily constant the steady state solution for the proton flux is:

$$N_p(E) = \frac{\sigma^0_{01}(E)}{\sigma^0_{10}(E)} \cdot N_H(E)$$

The resultant proton flux is given by the hydrogen flux and the ratio of the cross sections only. This ratio can be approximated within the energy range 0.25— 1.0 MeV

$$R^0(E) = \frac{\sigma^0_{01}(E)}{\sigma^0_{10}(E)} = 2200 \cdot E^{2.77}, \quad \text{with } E \text{ as always in MeV}.$$

In order to find a differential proton flux at low altitudes of

$$N_p(E) = 7 \cdot E^{-3} \quad \text{p/cm}^2 \text{ sec ster MeV},$$

which is an approximation of the observed equatorial differential proton flux that is good for the lower energy range only, a differential fast hydrogen flux of

$$N_H(E) = \frac{N_p(E)}{R^0(E)} = 3.18 \cdot 10^{-3} \cdot E^{-5.77} \quad \text{H*/cm}^2 \text{ sec ster MeV}$$

is necessary.

This finally leads to the proton flux at the maximum of the distribution in the outer belt at $L = 3$ that is necessary to sustain the observed proton flux at low L-values of:

$$j_\perp(E) = 4 \cdot 10^7 \cdot E^{-0.07} \quad \text{p/cm}^2 \text{ sec ster MeV}.$$

Apparently no substantial energy dependence within the energy range 0.25 to 1.0 MeV for the protons of the outer belt is required. Due to the approximations employed this is not exactly so, especially as the approximation of the measured proton spectrum by a power law spectrum ~E^{-3} is good only in the lower energy range whereas the spectrum becomes steeper with higher energies indicating that the outer belt proton spectrum should fall off also. Still, for the energy range 0.25 to 0.5 MeV the result is related to the fact that the outer belt proton spectra are peaked somewhere in this energy range with the exact point of the peak depending on the *L*-value and in the *L*-range that contributes most to the H* flux. More important is the fact that the proton flux necessary for maintaining the proton population of the low altitude belt is of reasonable magnitude as compared with measurements of DAVIS and WILLIAMSON [1963] and the measurements of Mihalov and WHITE [1966] which have to be extrapolated to the equator as these were taken at *B* = 0.10
Gauss.

Performing the calculations for different equatorial *L*-values reveals a slight dependence of the absolute flux on *L* as is shown in fig. 5 normalized to *L* = 1.1. This *L*-dependence in the calculation can not be seen in the actual measurements. It results from the diminishing shadowing of the H* flux by the solid earth and should be seen in the measurement also, if there are no mechanisms that counteract the effect; these will have to be looked for in the changing composition of the atmosphere with height.

So, the first result is that the proton content of the outer belt indeed is sufficient to maintain the observed proton fluxes at low altitudes through the mechanism proposed. It should be pointed out that the low attitude belt described should not be

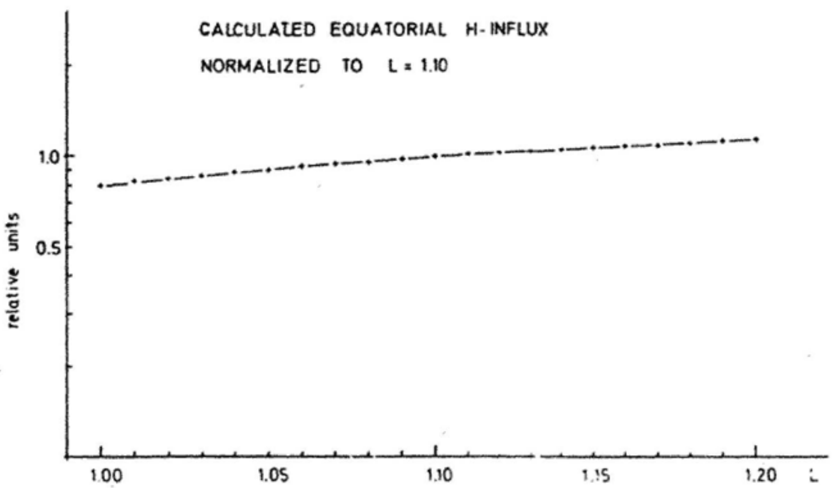

Fig. 5: The calculated equatorial H* - influx perpendicular to *B* resulting from the outer belt proton distribution of fig. 4 at different *L*-values. The H* fiux is set to 1 for L=1.1.

confined to these low altitudes, but is just difficult to measure at greater heights as the high intensity of the stable trapped high energy protons interferes with the measurement [MORTTZ 1971].

Also the pitch angle distribution to be expected for the low altitude protons has been calculated using two different procedures. First the influx of H* at a low L point at the equator for different angles of incidence with the magnetic field vector has been calculated by the same procedure of numerical integration over the outer belt as for the H* flux leading to the equatorial mirroring protons. Second the influx of H* at the mirror point corresponding to the equatorial pitch angle was calculated. This influx should give rise to a mirroring proton population there.

The results of these two approaches differ only slightly with the resulting proton flux at the mirror point being typically slightly lower than the flux at the equator with the corresponding equatorial pitch angle. An in-between value for the pitch angle distribution is expected because a proton generated near the equator with a pitch angle less than 90 degrees will encounter a slightly higher atmospheric density in its bounce motion, while a proton generated at an off-equatorial mirror point encounters a slightly lower atmospheric density. The resultant pitch angle distributions for a point $L = 1.1$, $B = B_0$ are shown in fig. 6. The conclusion is that indeed the source mechanism proposed leads to a high pitch angle anisotropy for the protons at low L-values. This anisotropy is nearly independent of height in agreement with the measurements.

Finally several low altitude equatorial satellite passages have been computer simulated taking as input the L and B values of the point of the actual measurement and calculating the flux at these points relative to the maximum flux at the $B=B_0$ equator passage. For comparison with the actual measurements the integral flux

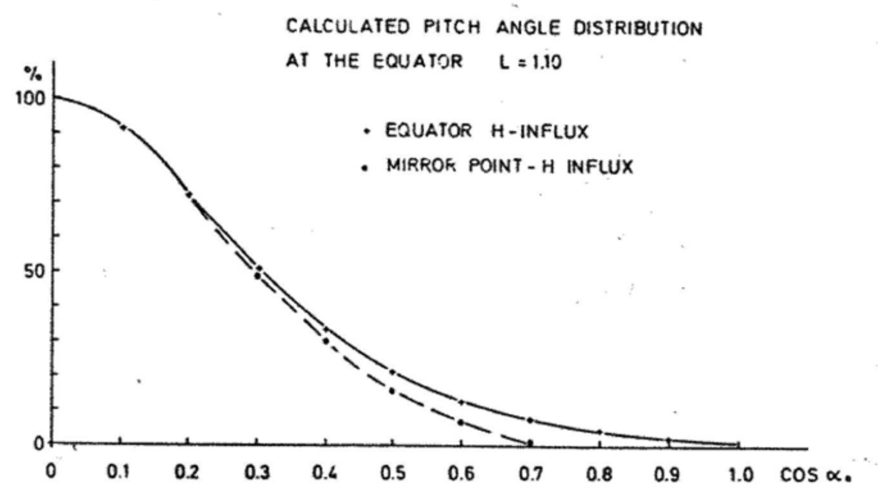

Fig. 6: The pitch angle distributions at an equatorial point of $L = 1.1$ derived at by the two approaches described in the text.

of the calculated distribution was normalized to the integral count rate of the actual measurement. The results for two passages are shown in fig. 7 and 8. They give an excellent agreement of the theory with the measurements.

Discussion

With fairly simple assumptions it is possible to explain a measurement that is surprising at first sight. Several refinements can be introduced which should lead to a more exact quantitative model.

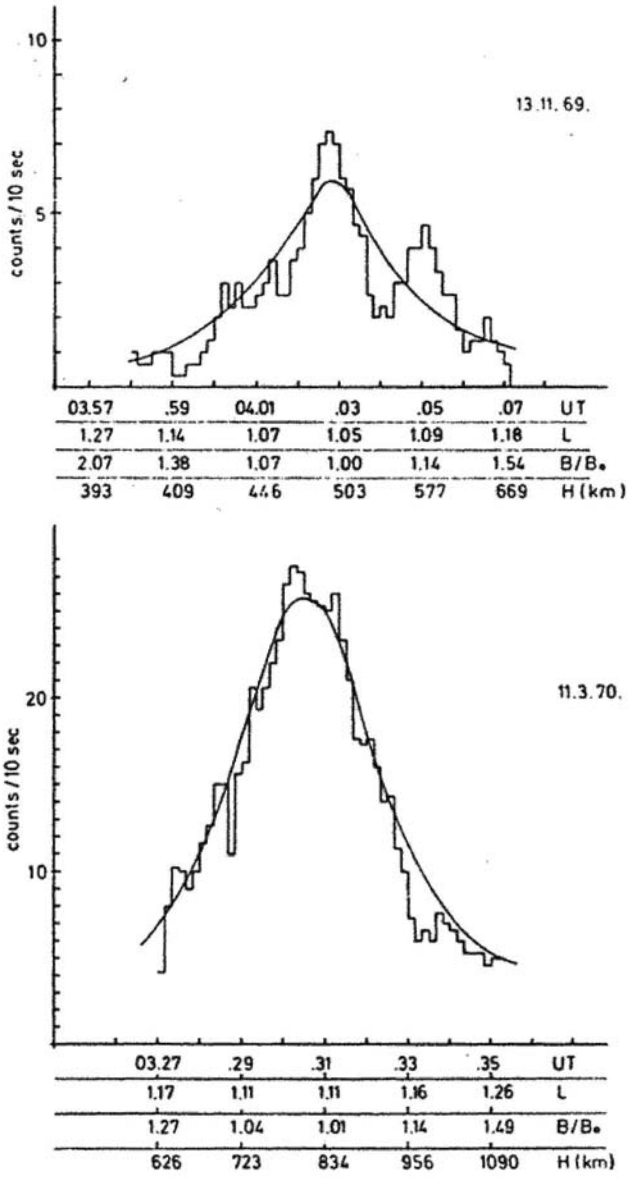

Fig. 7 and 8: Comparisons of actual count rate profiles (channel 3) from two low altitude equatorial passes of the satellite with the results of computations. The count rates have been smoothed by averaging the count rate of each 10 sec cycle with the count rates of the two neighbouring cycles.

1. Loss of the population and alteration of the spectrum through ionization losses should be included.

2. The generation of protons through charge exchange with the other atmospheric constituents which have other cross section ratios and other absolute values than Oxygen should be considered. This will influence the proton intensity as the relative abundances of the atmospheric constituents vary. Especially the fact that the increase of the equatorial H* influx by about 30 % going from L = 1 to L = 1.15 is not reflected in the proton measurements should be explained. Overall the inclusion of other atmospheric constituents should lead to a slightly lower proton flux in the outer belt that is necessary for maintaining the low altitude proton belt.

3. A more refined model of the outer belt proton distribution could be used.

There are some predictions that can be derived from this model.

1. The proton population should be present at all local times and thus constitute a real radiation belt. In the present case it could be observed at local morning and evening hours only, as other local times were not accessible to the satellite.

2. There should be a correlation with the exospheric thermal hydrogen density variations.

3. There should be a slight longitudinal dependence along a certain L-shell. In the present analysis all effects of a proton drift have been neglected. The possibility to drift obviously depends on the proton lifetime and thus on the atmospheric density. Allowing for a certain drift one is lead to the interesting result that — as long as the H* influx is not depleted - the proton intensity on a certain L-shell should depend on whether this L-shell at the point in consideration gains or loses in height following the proton drift direction. Thus the highest proton intensities on a certain L-shell should be seen shortly west of the South Atlantic Anomaly. This is so because the protons there are generated at a higher atmospheric density than they encounter on their subsequent drift path. The present measurements are not of sufficient sta tistical significance to reveal this effect.

4. The low altitude proton belt should respond to intensity variations in the outer belt due to the strong coupling of the two phenomena.

This last effect has actually been seen in the present experiment.

During and following the large magnetic storm event commencing March 8, 1970 an increase in the low energy proton population was observed in the outer radiation belt. This increase (at high B/B_0 values where it could be observed with this experi ment) depends on the L-shell and the proton energy. The highest increases were registered at the lowest energies and at L = 3, the L-shell that gives the relatively highest contribution to the low altitude belt. Following the magnetic storm, during the first observed low altitude equatorial pass of the satellite on March 11, a higher proton intensity was also registered in the low altitude beit. This pass is the one shown in fig. 8. Compared with the last passage before the magnetic storm occurred, the intensity is increased by a factor of 4.5 in the overall energy range 0.25 — 1 .65 MeV. Fig. 9 gives the spectra of these two passes which also show the relativly higher increase at lower energies in agreement with measurements in the outer belt.

As the lower belt integrates over the whole outer belt it is difficult to give a simple quantitative correspondence of the intensity increases in the outer belt to the increase in the low altitude belt but the strong coupling shows clearly. This is seen clearly from the overall intensity variations with time for the two regions of space shown in fig. 10. Here the count rate versus time in the low altitude belt is compared to the count rate at a *B, L* - point in the outer belt. Without the coupling of the low altitude belt to the outer belt the long time persistency of an increased intensity at low altitudes and correspondingly short lifetimes will hardly be explainable.

The intensity increase observed and its time persistency are believed to be a strong argument in favor of the proposed source mechanism.

Conclusions

There exists an energetic proton radiation belt at low altitudes closely concentrated around the $B = B_0$ equator. This low altitude belt is believed to consist of protons that come from the outer Van Allen Belt travelling the distance between the two regions as fast hydrogen neutrals unbothered by the earth's magnetic field. As the

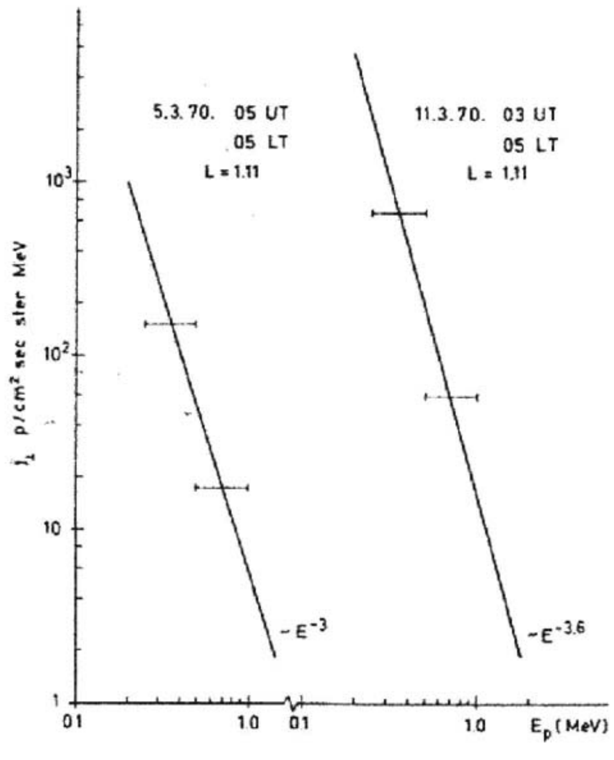

Fig. 9: Comparison of differential proton spectra measured in the low altitude belt shortly before and shortly after the magnetic storm event commencing March 8, 1970.

low altitude belt is a copy of the outer belt with intermediate processes that favor lower energies, the energy range of the telescope EI-92 is favorably adapted to studying this low altitude belt. It should be interesting to extend research to lower energies, especially as it is expected that the large intensities of low energy protons forming the ring current during the main phase of a magnetic storm should also be projected into the regions of the low altitude belt.

Finally this mechanism might be an explanation for the high intensities of low energy protons that have been measured at low altitudes on the night side of the magnetosphere only [FREEMAN 1962, HILTON et al. 1966] as here the main asymmetry for the described belt should be introduced for keV protons by the magneto-spheric tail as an abundant source for low energy protons.

Acknowledgements

It is a pleasure to thank Drs. HOVESTADT, SCHOLER and HÄUSLER of the Max-Planck-Institut für Extraterrestrische Physik in Garching for many discussions on

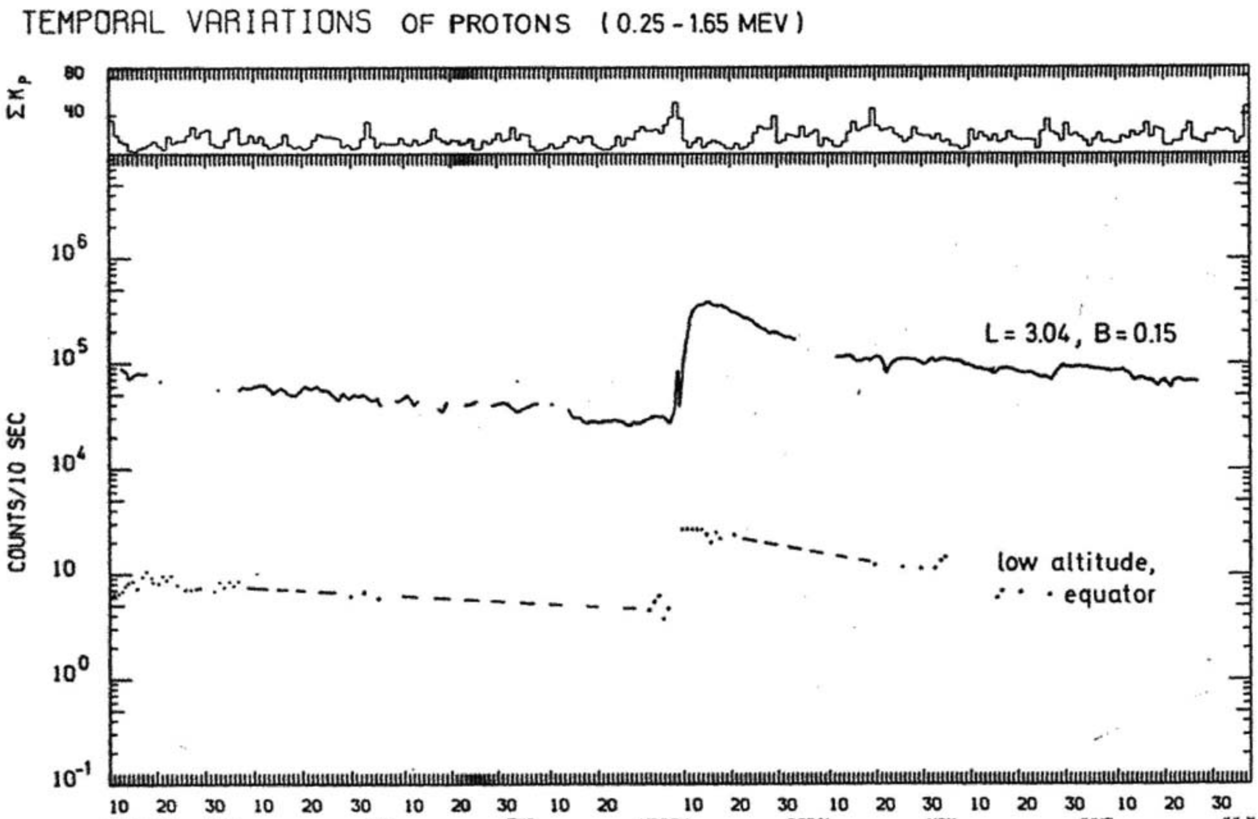

Fig. 10: Comparison of the long-term temporal variations in the count rates of channel 3 (E_p: 0.25-1.65 MeV) for a point in the outer radiation belt (L = 3.04 ±0.07, B = 0.150±0.010 Gauss) and within the low altitude belt.

the measurements. I also thank my colleagues of the institute in Kiel with who I first discussed the source idea, especially J, SCHMIDT, who is an expert on atmospheric phenomena, and R. MÜLLER, who made the computer time available and gave some valuable assistance in the computer work,

I gratefully appreciate Dr. PIEPER'S critical reading and commenting on the first manuscript.

This work was supported by the German "Bundesministerium für Bildung und Wissenschaft" under grant WRK 63.

References

DAVJS, L. R., J. M, WILLIAMSON: Low-energy trapped protons. Space Res, 3, 365, 1963

FREEMAN, J, W.: Detection of an intense flux of low-energy protons or ions trapped in the inner radiation zone. J. Geophys. Res. 67, 921, 1962

HILTON, H.H., J.R, STEVENS and A.L. VAMPOLA: Measurements of fluxes of low energy protons and electrons with a Faraday Cup detector, in Aerospace Corp, Report SSD-TR-66-41, Compilation of Scientific Results from the SSD/Aerospace Pll Radiation Monitoring Satellite 1964-45a, 1966

HOVESTADT, D.: Private communication, 1971

HOVESTADT, D., B. HÄUSLER, and M. SCHOLER: Observation of energetic particles at very low altitudes near the geomagnetic equator, Preprint 1972, submitted for publication to Phys. Rev, Letters

KING, J. H.: Models of the trapped radiation environment. Volume IV: Low energy protons, NASA SP-3024, 1967

MEIER, R.R.: Observations of Lyman-α and the atomic Hydrogen distribution in the thermosphere and exosphere. Space Res, 10, 572, 1970

MIHALOV, J. D. and R. S. WHITE: Low-energy proton radiation belts, J, Geophys. Res. 71, 2207, 1966

MORITZ, J.; Measurements of radiation belt protons in the energy range 0.25 to 1.65 MeV onboard the Satellite "Azur", Z. Geophys. 37, 179, 1971 (in German)

TOBUREN, L. H., M. Y. NAKAI and R. A. LANGLEY: Measurement of high energy charge-transfer cross sections for incident protons and atomic Hydrogen in various gases. Phys. Rev. 171, 114, 1968